Accepted Manuscript

Effect of planetary ball milling on physicochemical and morphological properties of sorghum flour

Pablo Martín Palavecino, María Cecilia Penci, Pablo Daniel Ribotta

Effect of planetary ball milling on physicochemical and morphological properties of sorghum flour

Pablo Martín Palavecino[1,2]; María Cecilia Penci[1,2]; Pablo Daniel Ribotta[1,2,3]

[1] CONICET-UNC. Instituto de Ciencia y Tecnología de Alimentos Córdoba (ICYTAC), Argentina.

[2] Universidad Nacional de Córdoba; Facultad de Ciencias Exactas, Físicas y Naturales; Instituto de Ciencia y Tecnología de los Alimentos; Córdoba, Argentina.

[3] Universidad Nacional de Córdoba. Instituto Superior de Investigación, Desarrollo y Servicios en Alimentos, SeCyT. Argentina.

Corresponding author: Ph.D. Pablo Daniel Ribotta; Tel: + 54 351 462 9520

E-mail address: pdribotta@unc.edu.ar.

13 **ABSTRACT**

14 Planetary ball milling was applied to white sorghum flour with the aim of modifying its thermal,

15 structural and morphological properties. Median particle size decreased from 57.2 μm a 20.8

16 μm with increasing milling energy. Particle size-energy models indicated that only part of the

17 energy was used for developing new surfaces. Abrasion of starch granules could be observed

18 by SEM and the increment of damaged starch levels. Gelatinization temperatures measured by

19 DSC were not affected by the process (T_p average 73.4±0.4 °C); yet, gelatinization enthalpy

20 (ΔH) and crystallinity degree (determined by WAXS) decreased with increasing milling energy

21 from 5.54 J/g and 28% to 2.98 J/g and 17.0%, respectively. Then, some pasting parameters

22 significantly changed: final viscosity (from 3947 to 3535 cP) and, consequently, setback (from

23 2339 to 1896 cP). Planetary ball milling significantly changed the functional properties of

24 sorghum flour and suggested that this method is an alternative to widen sorghum flour food

25 applications.

28

29 **1. Introduction**

30 Consumers are increasingly demanding food produced from sustainable and non-GMO crop.

31 Then sorghum is ideal since its hybrids can grow in salty or sandy soils with low amounts of

32 water, fertilizer and pesticides. Although sorghum is the fifth cereal crop produced worldwide,

33 most of African and Asian production is consumed directly as food and the production of USA

34 and Latin America is used as animal feed (Bedford et al., 2017; Léder, 2004). The nutritional

35 properties of sorghum lie in its high amount of starch, phenolic acid and flavonoid; nevertheless,

36 this cereal is not important in the commercial food systems (Hager, Wolter, Jacob, Zannini &

37 Arendt, 2012). The most usual method to produce sorghum flour around the world involves

38 partial dehulling followed by dry milling, since this allows a low-fiber product and avoids the

39 drying process after the wet milling procedure (Sun et al., 2014). Also, the wastewater treatment

40 should be considered despite the high efficiency and the great number of alternatives for

41 bioreactors (Sepehri and Sarrafzadeh, 2018).

42 The improvement of sorghum flour properties could allow the introduction of this cereal to the

43 food industry and, therefore, to human diets around the world. In this sense, there has been a

44 growing interest over the past few years in physical methods to enhance the functional

45 properties of flour as they increase their applications without resorting to chemical reagents. This

46 turns them into environmentally friendly methods with wider acceptance by consumers. Among

47 these treatments, recent modifications were carried out with high hydrostatic pressure,

48 ultrasound, pulsed electric field and microwaves (Ashogbon and Akintayo, 2014). In turn, simpler

49 methods like particle-size classification and fine grinding were the most common modification

50 strategies to improve gluten-free products (Gómez and Martínez, 2016).

51 Planetary ball milling is an innovative technology with successful applications in pharmaceutical

52 and nanomaterial industry. However, only few advances were made in food development. This

53 technology can improve material characteristics without producing hazardous materials. Ball

54   milling applied to flour can modify starch structure and behavior (Delogu, Gorrasi & Sorrentino,

55   2017; M. Loubes & Tolaba, 2014; Shan et al., 2016). Particularly, milling processes like abrasive

56   milling and planetary ball milling have modified crystallinity and, consequently, water absorption,

57   thermal parameters and rheological behavior of amaranth starch-enriched fraction (Roa,

58   Santagapita, Buera & Tolaba, 2014). Liu et al. (2011) and González et al. (2018) found that

59   intense grinding in wheat starch granules decreased enthalpy and temperature of gelatinization

60   and increased soluble material loss as a result of slight depolymerization of amylose and

61   amylopectin.

62   Grinding modeling aims at building mathematical relationships between feed and product

63   particle sizes that allow mill and grinding system designs. From this, different design and

64   modeling methods have been developed to achieve effective results by simple methods (Austin

65   & Concha, 1994; Mio, Kano & Saito, 2004).

66   The aim of the present work was to evaluate the effects of planetary ball milling on the

67   physicochemical and morphological properties of sorghum flour and model its relationships.

68

69

2. Materials and methods

2.1. Materials

Partially dehulled white sorghum flour from Pannar-8706 W hybrid grown in central region of Argentina was provided by Amylum S.A. (Córdoba, Argentina). The moisture content of the flour was 11.4% and its composition on a dry basis was: lipid 5.4%, ash 1.2%, protein 7.9% and total carbohydrates 85.5% (76.0% starch).

All chemicals were analytical reagent grade and all solutions were prepared by using deionized water.

2.2. Sorghum flour ball milling

The flour was dry ground using a planetary ball mill (PM-100, Retsch, Germany) with five times mass of zirconium oxide balls (5 mm diameter). The jar rotation speed was set at 400 rpm with a change in direction of rotation every 30 seconds and 40-minute breaks every 10 minutes of treatment (to prevent temperature from exceeding 55°C). The grinding energy was set at five levels, considering that the milling power is delivered practically constant for certain conditions, the samples differs in treatments time (Table 1). Because the energy was applied to sample and balls, previous calibration with an empty jar were carried out.

After each treatment moisture content was determined according to the standard method (AOAC, 2000), varying from 11.2% to 8.9%, for 0.26 kJ/g and 5.84 kJ/g, respectively.

2.3. Particle-size distribution

Particle-size distribution of samples was measured with a laser particle-size analyzer (LA-960, Horiba Instruments, USA). Samples were analyzed with the liquid sampler and both circulation velocity and agitation were set at level 10 (out of 15). The sample refractive index was 1.54 and 1.33 for the dispersant. Size distribution parameters Dv_{50} (median), Dv_{10} and Dv_{90} (particle

93 diameters where cumulative volume of particles are 10% and 90%, respectively), mode and

94 mean were measured and expressed in volumetric base. Span was calculated as $(Dv_{90} - Dv_{10})/$

95 Dv_{50}. Measurements were carried out in triplicate.

96 *2.4.   Milling modeling*

97 The energy supplied per unit of processed mass to produce a small change in particle size can

98 be expressed as a function of the power law type, which is a general interpretation of several

99 laws presented by different authors and known as the general law of milling (Snow, Allen, Ennis

100 & Litster, 1999) (Eq. 1).

101 $$\frac{dE}{dx} = -\frac{C}{x^n} \quad (1)$$

102 where E is the applied energy, x is a selected particle size dimension, and n and C are constants

103 related to the material. Size parameter mean, median, Dv_{10} and Dv_{90} data were fitted to the

104 integrated form of Eq. 1 (Eq. 2).

105 $$E = \frac{C}{1-n}(x_f^{1-n} - x_i^{1-n}) \quad (2)$$

106 Where x_i are the initial mean, median, Dv_{10} or Dv_{90} and x_f represents size parameter at different

107 treatment times.

108 Fitness of fracture to a first-order kinetics was also evaluated with the model proposed by Mio,

109 Kano y Saito (2004) (Eq. 3).

110 $$\frac{D_t}{D_0} = \left(1 - \frac{D_l}{D_0}\right)e^{-Kt} + \frac{D_l}{D_0} \quad (3)$$

111 where D_t, D_0 and D_l are the values of the mean at time t, time 0 and milling limit time, respectively,

112 and k is the fracture velocity constant.

113 *2.5.   Scanning electron microscopy (SEM)*

114   A scanning electron microscope (Sigma, Carl Zeiss, Germany) was used to evaluate the

115   morphology of flour particles, mainly starch granules. Samples were coated with gold and

116   images were taken at an electron acceleration of 3 kV under high vacuum conditions with main

117   and secondary detectors at different magnifications.

118   *2.6.   Damaged starch*

119   Damaged starch (DS) levels were estimated following the methods 76-30A and 80-60 (AACC,

120   2000). The amount of DS was expressed as percentage of starch subject to enzymatic

121   hydrolysis in the sample, as the mean of two duplicates.

122   *2.7.   Water absorption*

123   Water absorption (WA) of flour was determined following Yousif et al. (2012) procedure. Briefly,

124   samples (500±5 mg db) were suspended into water (6 mL), incubated at 25 °C for 30 minutes

125   and then centrifuged, and the supernatant was discarded. The WA determination was performed

126   in triplicate and the mean was expressed as g of absorbed water by g of sample.

127   *2.8.   Thermal properties*

128   Thermal properties were evaluated with a differential scanning calorimeter (DSC 823e, Mettler

129   Toledo, Switzerland) controlled by STARe software. Aluminum pans of 100 μL were filled with

130   10 mg db of flour and 20 μL of deionized water, and then hermetically sealed. The heating ramp

131   was set with a rate of 10 ºC/min from 20 to 120 ºC. The parameters assessed in the thermograms

132   were: onset (T_o), peak (T_p) and conclusion temperatures (T_c), gelatinization enthalpy (ΔH, J/g

133   of flour) and peak width and height. Thermal properties were evaluated in duplicate and the

134   results expressed the mean.

135   *2.9.   Pasting properties*

136 Pasting parameters were determined with a Rapid Viscosity Analyzer (RVA 4500, Perten

137 Instruments, Australia) 10% w/w of flour in water. The temperature profile consisted in a holding

138 period at 50 ºC (1 min), heating to 95 ºC (4 min), holding at 95 ºC (2.5 min) and finally cooling

139 to 50 ºC (3 min) and maintaining (2 min). Stirring speed was 960 rpm for the first 10 s and 160

140 rpm until the end of the assay. Thermocline software (V 3.15, Perten Instruments, Australia) was

141 used to control the device and acquire the data to obtain pasting parameters: pasting

142 temperature (PT), peak viscosity (PV), trough viscosity (TV), final viscosity (FV), breakdown

143 (BD=PV−TV) and setback (SB=FV–TV). Pasting profile determination were carried out in

144 duplicate.

145 *2.10.   Wide-Angle X-ray Scattering*

146 WAXS was carried out with an X-ray diffractometer (PW-1800, Philips, USA) using 40KV and

147 30mA radiation to scan from 2 to 30º with time steps of 0.02º/2.5 s. The crystallinity degree (CD)

148 is the ratio of crystalline/amorphous phase and was calculated with Peakfit software v4 (Jandel

149 Scientific, USA) through diffractogram deconvolution (Ribotta, Cuffini, León & Añon, 2004). The

150 diffractograms were obtained in duplicate for each sample.

151 *2.11.   Statistical analysis*

152 Analyses of variance (ANOVA, multiple comparison test by DSG, α=5 %) were performed using

153 InfoStat software (Version 13p, Di Rienzo et al. 2011) and artwork was made using Excel (2016

154 version, Microsoft).

155

3. Results and discussions

3.1.   Particle-size distribution changes and modelling

Particle-size distribution of sorghum flour samples was significantly modified by planetary ball milling. Figure 1 shows the particle-size distribution of each sample, where untreated flour (0) has two particle populations forming a bimodal curve with peaks at 18 and 152 µm. Treatments produced a new population of particles with a local maximum at around 100 µm, which remained relatively invariant with the process time at approximately 5% v/v until maximum treatment time. Likewise, the 152 µm decreased and 18 µm increased with applied milling energy with highly milled sample (5= 5.84 kJ/g) showing a predominant particle population with a peak at 18 µm.

The starch fraction was isolated from the untreated flour following the procedure of Pérez Sira and Lares Amaiz (2004). Sorghum starch fraction showed a monodisperse distribution with a mean of 16 µm, which indicated that the milling treatment breaks the flour particles into separated starch granules.

The mean particle size decreased with the increase in applied energy from 86.6 µm to 36.0 µm (Table 1). In turn, the span (particle size dispersion) oscillated slightly around 3.3 indicating a very wide dispersion in all samples. It can also be observed that the median was considerably lower than the mean for all cases, highlighting their asymmetry. Roa et al. (2014) found similar results for amaranth flour treated in the same mill, although in that case the span was reduced slightly but significantly.

Modeling of the milling procedure helped to understand the process and settle a base to its scale-up. The mean, median, Dv_{10}, and Dv_{90} were fitted to Eq. 2 and mean obtained the best regression (R^2 = 0.98). The *n* value from this equation is related to the new surface generation efficiency during the milling process (Roa et al., 2014a), and when *n* = 2 the equation correspond to the Rittinger model where energy is proportional to the new surface produced (Snow et al.,

180   1999). The n value found was 2.44, indicating that only a fraction of the applied energy was used

181   to generate new surfaces; hence, another part was probably dissipated as thermal energy,

182   elastic collisions with fiber particle or particle abrasion. The proportionality constant of the Eq. 2

183   (C) obtained was 1954 kJ g^{-1} μm^{n-1}. This parameter varies with milling conditions, ball loading

184   and sizes, and indicates how many energy is used to produce the size reduction and new surface

185   creation, therefore an investigation of the optimal milling conditions should aim to minimize this

186   value (Snow et al., 1999; Xu and Wang, 2017).

187   The experimental data were also adjusted by Eq. 3, reaching a R^2 of 0.98 which proved the first-

188   order kinetics with a K of 0.014 min^{-1} and D_l of 27.1 µm. These values indicated a rapid decrease

189   of the normalized media (D_t /D_0) at the milling initial stage and a stabilization close to the mean

190   of the highly treated sample. Mio et al. (2004) reported similar behavior in planetary ball milling

191   for several devices and milling conditions. These authors also stated a close relationship

192   between K and specific milling energy particularly useful for simulation and scale-up.

193   The good fit found for Eq. 3 should be highlighted, since, in this case, the samples do not comply

194   with some of these models assumptions: the start material should be monodisperse and

195   significantly larger than the resulting ones; in addition, most models were developed to weigh

196   particle distributions rather than volumetric (Verkoeijen, A. Pouw, M. H. Meesters & Scarlett,

197   2002).

198

199   *3.2.   Morphologic characterization*

200   The morphology of untreated and highly treated flour is shown in Fig. 2. In the microscopic

201   images of sorghum flour polyhedral and oval starch granules, globular protein bodies and fiber

202   particles could be observed.

203 From the images acquired by SEM it was possible to observe the breakage of flour particles and

204 the increase of the modification produced in the surface of the starch granules. The planetary

205 milling process produced not only the fracture of flour particles, it also changed starch granule

206 and, therefore, structural, absorptive, thermal and rheological properties. These transformations

207 are summarized in Tables 2 and 3 and will be discussed in the next sub-sections.

208 Untreated sample (Fig. 2-0A) shows large particles (close to 100 μm), not founded in highly

209 treated sample (Fig. 2-5A). Endosperm fragments, starch granules, fiber particles and protein

210 bodies forming a conglomerate can be observed at a higher magnification (Fig. 2-0B), as

211 described by other authors (Belton and Taylor, 2002; Hager et al., 2012). However, after the

212 most extensive treatment (Fig. 2-5B), granules were no longer attached to each other, no large

213 fiber particles were observed and protein bodies were disintegrated.

214 In turn, starch granule showed evident damage by planetary mill grinding (Figure 2-5C and D):

215 surface changed from smooth to rough, most of the granules being distorted. Similar results

216 were described by Barrera et al. (2013) for wheat starch treated with a disc mill and Liu et al.

217 (2011) for ball milled maize, highlighting that starch damage could be observed in granules from

218 different sources and through diverse milling devices.

219 *3.3.   Damaged starch*

220 The milling models focused on the mechanisms of division and fracture, but not on abrasion. In

221 this case, since the treated material is a cereal flour, a large part of the abrasion effect could be

222 known by investigating the damaged starch content. The damaged starch (DS) is quickly

223 hydrolyzed by α-amylases representing an important transformation produced by ball milling

224 since damaged starch generally influences water absorption, thermal properties and rheological

225 behavior (Barrera et al., 2013a; León et al., 2006).

226 The initial level of DS (5.2%) was produced by the industrial hammer mill during flour production

227 process and planetary ball milling increased starch damage up to 17.9 % (Table 2).

228 The effect of the applied energy on the damaged starch content was investigated. These

229 parameters were adjusted to an exponential equation (Eq. 4) with a high fitting coefficient

230 (R^2=0.987). This fitting indicated that the stronger the treatments, the less energy was needed

231 to generate the same change in the amount of damaged starch. For example, between

232 treatments 1 and 2, 0.73 kJ/g was needed to produce a difference of 0.7 % of DS, whereas

233 between points 4 and 5 the application of 2.91 kJ/g produced an increase of 7.8 % in DS.

234 $$DS(\%) = 5{,}4\, e^{0{,}2\, E} \qquad (4)$$

235 *3.4.   Water absorption*

236 The water absorption results were summarized in Table 2 and a slight increase in WA was

237 observed with the application of higher milling energy. The highly treated sample showed the

238 highest water retention capacity, 15 % more compared with the untreated flour.

239 This increment in the water intake could be explained by the damaged starch generated during

240 the milling process and was reflected in a positive correlation between these parameters (r=0.99,

241 p<0.05). The damaged granules possess greater affinity for water and depending on its botanical

242 source (which determines the granule size, pores and shape) a damaged granule could absorbs

243 water up to 3 times than native ones (Liu et al., 2011; Roa et al., 2014b).

244 In turn, Loubes and Tolaba (2014) reported a strong increase of WA in planetary milled rice flour

245 probably related to higher rotational speed and final temperature reached in the processing

246 compared to those used in this study.

247 *3.5.   Thermal properties*

248 The gelatinization enthalpy (ΔH) decreased with increasing milling energy (Table 2), in

249 agreement with results published by other authors for wheat, amaranth and rice samples

250 (Barrera, León & Ribotta, 2012; M. Loubes & Tolaba, 2014; Roa, Baeza & Tolaba, 2015).

251 It was previously demonstrated (Barrera et al., 2013a) that highly damaged starch granules

252 absorb water quickly and leach not only amylose but also amylopectin, giving the ability to

253 hydrate spontaneously in cold water, such as pre-gelatinized starch. Due to these changes

254 damaged starch and the starch granules fragments partially contribute to the endothermic

255 gelatinization energy (Barrera et al., 2012). The reduction of ΔH and peak height values (Table

256 2) found in this study could be attributed to partial destruction of the starch structure.

257 On the other hand, gelatinization temperatures were not significantly affected by planetary

258 milling (T_o= 67.2±1.1 °C, T_p= 73.4±0.4 °C and T_c= 80.4±0.4 °C), according to studies reported

259 by other authors for wheat starch with DS levels up to 23.8 % (Barrera et al., 2012). In turn, Roa

260 et al. (2015) found only significant differences in T_o for the most intensely treated samples by

261 planetary grinding of amaranth starch (6.52 kJ/g of applied energy) and González et al. (2018)

262 found a decrease in T_p for planetary ball milled rice starch.

263 *3.6.   Crystallinity degree*

264 Sorghum flour showed a crystalline structure type A, characteristic of cereals with strong

265 refractive peaks at 15° and 23° and a double at 17° and 18°, and no displacement of the peaks

266 was detected with the treatment (Figure 3). In addition, WAXS allowed determining crystallinity

267 loss during the planetary grinding process, in which CD decreased from 28.8 % to 17.0 % as

268 the treatment became more intense (Table 2). This loss in crystallinity and preservation of the

269 diffraction pattern was also reported by other authors for flour and starch with high content of

270 damaged starch, determined by x-ray diffraction and by NMR (nuclear magnetic resonance) (Liu

271 et al., 2011). An intense ball milling treatment produced changes in the crystalline phase and in

272   the crystallinity of polymeric materials which could led to its total amorphization (Delogu et al.,

273   2017). In this sense, Anzai et al. (2011) found that ball milled potato starch loss entirely its

274   crystalline structure and become amorphous after 17 hours treatment. Liu et al. (2011) reported

275   the disappearance of all the diffraction peaks of maize starch treated during 2 h in a ball mill and

276   reached 2.67% of CD after 3 h.

277   The gelatinization peak width showed a positive correlation with the damaged starch content

278   (r=0.85, p<0.05) and the peak height with the crystallinity degree (r=0.88, p<0.05). These results

279   indicate that the balls produce the partial disintegration of the crystals, formed mainly from

280   amylopectin, causing reduction of gelatinization enthalpy as was explained above.

281   *3.7.   Pasting behavior*

282   The heating of starch in excess of water produce the gelatinization of the granules (amylose

283   lixiviation and granule swelling) which increase the system viscosity and its subsequent cooling

284   results in a starch paste composite by a continuous phase of amylose chains with swollen

285   granules dispersed in it. The rapid viscosity analyzer (RVA) allows the assessment of the

286   viscosity evolution while the system was changing (Barrera et al., 2013a; Copeland et al., 2009).

287   Table 3 summarizes the pasting parameters of all samples and Fig. 4 shows the viscosity profile

288   of untreated and highly treated samples. Regarding the pasting parameters, final viscosity, and

289   consequently, setback showed significant differences between the samples. The PV and TV

290   showed slight differences between samples and breakdown was similar in all samples. In turn,

291   no differences were found for temperature and pasting time, exhibiting average values of

292   89.4±0.6 °C and 5.8±0.1 minutes, respectively. This indicates that at the beginning of the pasting

293   curve, behavior was similar in all samples, but differed in the cooling stage.

294   In the pasting curve a second peak can also be observed during cooling stage, which could be

295   ascribed to the presence of free fatty acids, following Zhang and Hamaker (2003, 2005). These

296 authors describe that samples stored for a certain time (2 months) show this behavior due to the

297 degradation of the lipids present in the flour. In addition, starch-lipid and starch-protein-lipid

298 complexes influence this behavior, varying with the content of fatty acids and the size of their

299 aliphatic chain. In our work, all samples exhibited similar behavior, probably because they were

300 stored during the same period of time and contained the same lipids.

301 The untreated sorghum flour sample showed a SB of 2339 cP that progressively decreased to

302 1896 cP for the maximum applied energy sample (5.84 kJ/g). Similar results were found by other

303 authors (González et al., 2018; Z. Zhang, Zhao & Xiong, 2010).

304 Final viscosity depends on several factors, such as the degree of amylose leached and the

305 volume and stiffness of the remaining granules. According to a previous work, higher starch

306 damage produced weaker and greater disintegration of the granules, and consequently, less

307 volume occupied by the disperse phase and more amylopectin in the continuous phase (Barrera

308 et al., 2013a). In this sense, the study published by Fu et al. (2018) on the thermal and structural

309 behavior of potato starch treated by ball grinding suggests that a small amount of remaining

310 crystals after gelatinization prevents retrogradation.

311 The FV showed a negative correlation with the applied energy (r=-0.83, p<0.05) in agreement

312 with the results reported by Loubes et al. (2018) which found that pasting parameters were

313 negatively affected by planetary ball milling time and speed.

314

315 **4. Conclusions**

316 The planetary milling process affected the particle-size distribution of sorghum flour, reducing

317 considerably its size at high levels of applied energy. In turn, planetary ball grinding significantly

318 affected the thermal and morphological properties of sorghum flour due to the partial destruction

319 of the starch granule structure. In this sense, the amount of damaged starch increased

320 significantly with the application of energy, which increased water absorption, decreased the

321 degree of crystallinity of the granule and hence decreased its gelatinization enthalpy.

322 Consequently, these changes caused differences in the pasting profiles, showing lower final

323 viscosities as the milling process became more intense. At the same time, the modelling results

324 indicated that, during milling, only a fraction of the applied energy was used to generate new

325 surfaces and that this followed a first-order kinetics. This shows that planetary grinding is a

326 suitable method for the production of modified flour, thus avoiding the use of chemical reagents

327 or water.

328

334

335

6. Bibliography

AACC, 2000. Approved Methods of the American Association of Cereal Chemists, 10th ed. St. Paul, USA.

Anzai, M., Hagiwara, T., Watanabe, M., Komiyama, J., Suzuki, T., 2011. Relationship between enthalpy relaxation and water sorption of ball-milled potato starch. J. Food Eng. 104, 43–48. https://doi.org/10.1016/j.jfoodeng.2010.11.025

AOAC, 2000. Official Methods of Analysis, 17th ed. Gaithersburg, MD, USA.

Ashogbon, A.O., Akintayo, E.T., 2014. Recent trend in the physical and chemical modification of starches from different botanical sources: A review. Starch/Staerke 66, 41–57. https://doi.org/10.1002/star.201300106

Austin, L., Concha, A., 1994. Diseño y simulación de circuitos de molienda y clasificación. Programa Iberoamericano de Ciencia y Tecnología.

Barrera, G.N., Bustos, M.C., Iturriaga, L., Flores, S.K., León, A.E., Ribotta, P.D., 2013a. Effect of damaged starch on the rheological properties of wheat starch suspensions. J. Food Eng. 116, 233–239. https://doi.org/10.1016/j.jfoodeng.2012.11.020

Barrera, G.N., Calderón-Domínguez, G., Chanona-Pérez, J., Gutiérrez-López, G.F., León, A.E., Ribotta, P.D., 2013b. Evaluation of the mechanical damage on wheat starch granules by SEM, ESEM, AFM and texture image analysis. Carbohydr. Polym. 98, 1449–57. https://doi.org/10.1016/j.carbpol.2013.07.056

Barrera, G.N., León, A.E., Ribotta, P.D., 2012. Effect of damaged starch on wheat starch thermal behavior. Starch - Stärke 64, 786–793. https://doi.org/10.1002/star.201200022

Bedford, D., Claro, J., Giusti, A.M., Karumathy, G., Lucarelli, L., Mancini, D., Marocco, E., Milo, M., Yang, D., 2017. Food Outlook, Food and Agriculture Organization of the United Nations. https://doi.org/ISSN 1560-8182

Belton, P.S., Taylor, J.R.N., 2002. Pseudocereals and Less Common Cereals. Springer Berlin

361   Heidelberg, Berlin, Heidelberg. https://doi.org/10.1007/978-3-662-09544-7

362   Copeland, L., Blazek, J., Salman, H., Tang, M.C., 2009. Form and functionality of starch. Food

363   Hydrocoll. 23, 1527–1534. https://doi.org/10.1016/j.foodhyd.2008.09.016

364   Delogu, F., Gorrasi, G., Sorrentino, A., 2017. Fabrication of polymer nanocomposites via ball

365   milling: Present status and future perspectives. Prog. Mater. Sci. 86, 75–126.

366   https://doi.org/10.1016/j.pmatsci.2017.01.003

367   Di Rienzo, J.A., Casanoves, F., Balzarini, M.G., Gonzalez, L., Tablada, M., Robledo, C.W.,

368   2011. InfoStat.

369   Fu, Z., Wu, M., Zhang, H., Wang, J., 2018. Retrogradation of partially gelatinised potato starch

370   prepared by ball milling. Int. J. Food Sci. Technol. 53, 1065–1071.

371   https://doi.org/10.1111/ijfs.13683

372   Gómez, M., Martínez, M.M., 2016. Changing flour functionality through physical treatments for

373   the production of gluten-free baking goods. J. Cereal Sci. 67, 68–74.

374   https://doi.org/10.1016/j.jcs.2015.07.009

375   González, L.C., Loubes, M.A., Tolaba, M.P., 2018. Incidence of milling energy on dry-milling

376   attributes of rice starch modified by planetary ball milling. Food Hydrocoll. 82, 155–163.

377   https://doi.org/10.1016/j.foodhyd.2018.03.051

378   Hager, A.-S., Wolter, A., Jacob, F., Zannini, E., Arendt, E.K., 2012. Nutritional properties and

379   ultra-structure of commercial gluten free flours from different botanical sources compared

380   to wheat flours. J. Cereal Sci. 56, 239–247. https://doi.org/10.1016/j.jcs.2012.06.005

381   Léder, I., 2004. Sorghum and Millets, in: Füleky, G. (Ed.), Cultivated Plants, Primarily as Food

382   Sources. Encyclopedia of Life Support Systems (EOLSS), Oxford ,UK, pp. 66–84.

383   https://doi.org/10.1002/9780470384923

384   León, A.E., Barrera, G.N., Pérez, G.T., Ribotta, P.D., Rosell, C.M., 2006. Effect of damaged

385   starch levels on flour-thermal behaviour and bread staling. Eur. Food Res. Technol. 224,

386   187–192. https://doi.org/10.1007/s00217-006-0297-x

387 Liu, T.Y., Ma, Y., Yu, S.F., Shi, J., Xue, S., 2011. The effect of ball milling treatment on structure

388   and porosity of maize starch granule. Innov. Food Sci. Emerg. Technol. 12, 586–593.

389   https://doi.org/10.1016/j.ifset.2011.06.009

390 Loubes, M., Tolaba, M., 2014. Thermo-mechanical rice flour modification by planetary ball

391   milling. LWT - Food Sci. Technol. 57, 320–328. https://doi.org/10.1016/j.lwt.2013.12.048

392 Loubes, M.A., González, L.C., Tolaba, M.P., 2018. Pasting behaviour of high impact ball milled

393   rice flours and its correlation with the starch structure. J. Food Sci. Technol. 55, 2985–2993.

394   https://doi.org/10.1007/s13197-018-3216-9

395 Mio, H., Kano, J., Saito, F., 2004. Scale-up method of planetary ball mill. Chem. Eng. Sci. 59,

396   5909–5916. https://doi.org/10.1016/j.ces.2004.07.020

397 Pérez Sira, E.E., Lares Amaiz, M., 2004. A laboratory scale method for isolation of starch from

398   pigmented   sorghum.   J.   Food   Eng.   64,   515–519.

399   https://doi.org/10.1016/j.jfoodeng.2003.11.019

400 Ribotta, P.D., Cuffini, S., León, A.E., Añon, M.C., 2004. The staling of bread: an X-ray diffraction

401   study. Eur. Food Res. Technol. 218, 219–223. https://doi.org/10.1007/s00217-003-0835-8

402 Roa, D.F., Baeza, R.I., Tolaba, M.P., 2015. Effect of ball milling energy on rheological and

403   thermal properties of amaranth flour. J. Food Sci. Technol. 52, 8389–8394.

404   https://doi.org/10.1007/s13197-015-1976-z

405 Roa, D.F., Santagapita, P.R., Buera, M.P., Tolaba, M.P., 2014a. Ball Milling of Amaranth Starch-

406   Enriched Fraction. Changes on Particle Size, Starch Crystallinity, and Functionality as a

407   Function   of   Milling   Energy.   Food   Bioprocess   Technol.   7,   2723–2731.

408   https://doi.org/10.1007/s11947-014-1283-0

409 Roa, D.F., Santagapita, P.R., Buera, M.P., Tolaba, M.P., 2014b. Amaranth Milling Strategies

410   and Fraction Characterization by FT-IR. Food Bioprocess Technol. 7, 711–718.

411   https://doi.org/10.1007/s11947-013-1050-7

412   Sepehri, A., Sarrafzadeh, M., 2018. Effect of nitrifiers community on fouling mitigation and

413   nitrification efficiency in a membrane bioreactor. Chem. Eng. Process. - Process Intensif.

414   128, 10–18. https://doi.org/10.1016/j.cep.2018.04.006

415   Shan, D., Deng, S., Zhao, T., Wang, B., Wang, Y., Huang, J., Yu, G., Winglee, J., Wiesner, M.R.,

416   2016. Preparation of ultrafine magnetic biochar and activated carbon for pharmaceutical

417   adsorption and subsequent degradation by ball milling. J. Hazard. Mater. 305, 156–163.

418   https://doi.org/10.1016/j.jhazmat.2015.11.047

419   Snow, R., Allen, T., Ennis, B., Litster, J., 1999. Size Reduction and Size Enlargement, in: Perry,

420   R., Green, D. (Eds.), Perry's Chemical Engineers' Handbook. McGraw-Hill, New York, pp.

421   20–23.

422   Sun, Q., Han, Z., Wang, L., Xiong, L., 2014. Physicochemical differences between sorghum

423   starch and sorghum flour modified by heat-moisture treatment. Food Chem. 145, 756–764.

424   https://doi.org/10.1016/j.foodchem.2013.08.129

425   Verkoeijen, D., A. Pouw, G., M. H. Meesters, G., Scarlett, B., 2002. Population balances for

426   particulate processes - A volume approach. Chem. Eng. Sci. 57, 2287–2303.

427   https://doi.org/10.1016/S0009-2509(02)00118-5

428   Xu, Y., Wang, Y., 2017. Size effect on specific energy distribution in particle comminution.

429   Fractals 25. https://doi.org/10.1142/S0218348X17500165

430   Yousif, E.I., Gadallah, M.G.E., Sorour, A.M., 2012. Physico-chemical and rheological properties

431   of modified corn starches and its effect on noodle quality. Ann. Agric. Sci. 57, 19–27.

432   https://doi.org/10.1016/j.aoas.2012.03.008

433   Zhang, G., Hamaker, B.R., 2005. Sorghum (Sorghum bicolor L. Moench) Flour Pasting

434   Properties Influenced by Free Fatty Acids and Protein. Cereal Chem 82, 534–540.

435   Zhang, G., Hamaker, B.R., 2003. A three component interaction among starch, protein, and free

436   fatty acids revealed by pasting profiles. J. Agric. Food Chem. 51, 2797–2800.

437   https://doi.org/10.1021/jf0300341

438 Zhang, Z., Zhao, S., Xiong, S., 2010. Morphology and physicochemical properties of

439   mechanically activated rice starch. Carbohydr. Polym. 79, 341–348.

440   https://doi.org/10.1016/j.carbpol.2009.08.016

441

442

443 **7. Tables**

444 Table 1. Experimental design and particle-size distribution parameters of planetary ball milled

445 sorghum flour.

Experiment	Milling time (min)	Energy (kJ/g)	Median (µm)	Mean (µm)	Dv$_{90}$ (µm)
0	0	-	57.2 [d]	86.6 [f]	202.9 [f]
1	5	0.26	66.4 [f]	83.3 [e]	193.8 [e]
2	20	0.99	58.4 [e]	76.0 [d]	178.5 [d]
3	40	1.96	34.0 [c]	58.15 [c]	134.9 [c]
4	60	2.93	27.8 [b]	52.5 [b]	118.8 [b]
5	120	5.84	20.8 [a]	36.0 [a]	82.5 [a]

446 Means with different letters within the same column indicate significant differences among samples (p<0.05).
447 Dv90 diameter corresponding to 90 % of cumulative volume

448

449

450 Table 2. Effects of milling energy on damaged starch (DS), thermal parameters (ΔH:

451 gelatinization enthalpy) and crystallinity degree (CD) of sorghum flour.

Treatment	DS (%)		WA		ΔH (J/g)		Peak height		Peak width		CD (%)	
0 (Control)	5.2	a	2.30	a	5.54	d	1.07	d	7.59	b	28.8	d
1 (0.26 kJ/g)	6.2	b	2.29	a	4.54	c	0.95	c	7.24	b	21.7	c
2 (0.99 kJ/g)	6.9	b	2.34	b	2.7	a	0.67	b	6.48	a	21.7	c
3 (1.96 kJ/g)	7.7	b	2.38	c	2.97	b	0.65	b	7.22	b	20.5	b
4 (2.93 kJ/g)	10.1	c	2.42	d	2.91	b	0.61	b	8.2	b	20.0	b
5 (5.84 kJ/g)	17.9	d	2.64	e	2.98	b	0.53	a	9.02	c	17.0	a

452 Means with different letters within the same column indicate significant differences among samples ($p<0.05$).
453

454

455   Table 3. Effect of planetary ball milling energy on pasting parameters (RVA) of sorghum flour.

Treatment	PV (cP)		TV (cP)		BD (cP)		FV (cP)		SB (cP)	
0 (Control)	2145	a	1608	a	537	a	3947	c	2339	c
1 (0,26 kJ/g)	2114	a	1572	a	542	a	4057	c	2485	c
2 (0,99 kJ/g)	2241	b	1685	b	556	a	3813	b	2128	b
3 (1,96 kJ/g)	2234	b	1663	b	571	a	3592	a	1929	a
4 (2,93 kJ/g)	2253	b	1670	b	565	a	3584	a	1914	a
5 (5,84 kJ/g)	2212	b	1639	b	573	a	3535	a	1896	a

456   Means with different letters within the same column indicate significant differences among samples ($p<0.05$). PV,

457   peak viscosity; TV, trough viscosity; BD, breakdown (PV-TV); FV, final viscosity; SB, setback (FV–TV).

458

Fig.1. Volume size distribution of planetary ball milled sorghum flour as a function of milling energy (0= no treatment, 1 = 0.26 kJ/g, 2 = 0.99 kJ/g, 3 = 1.96 kJ/g, 4 = 2.93 kJ/g, 5 = 5.84 kJ/g).
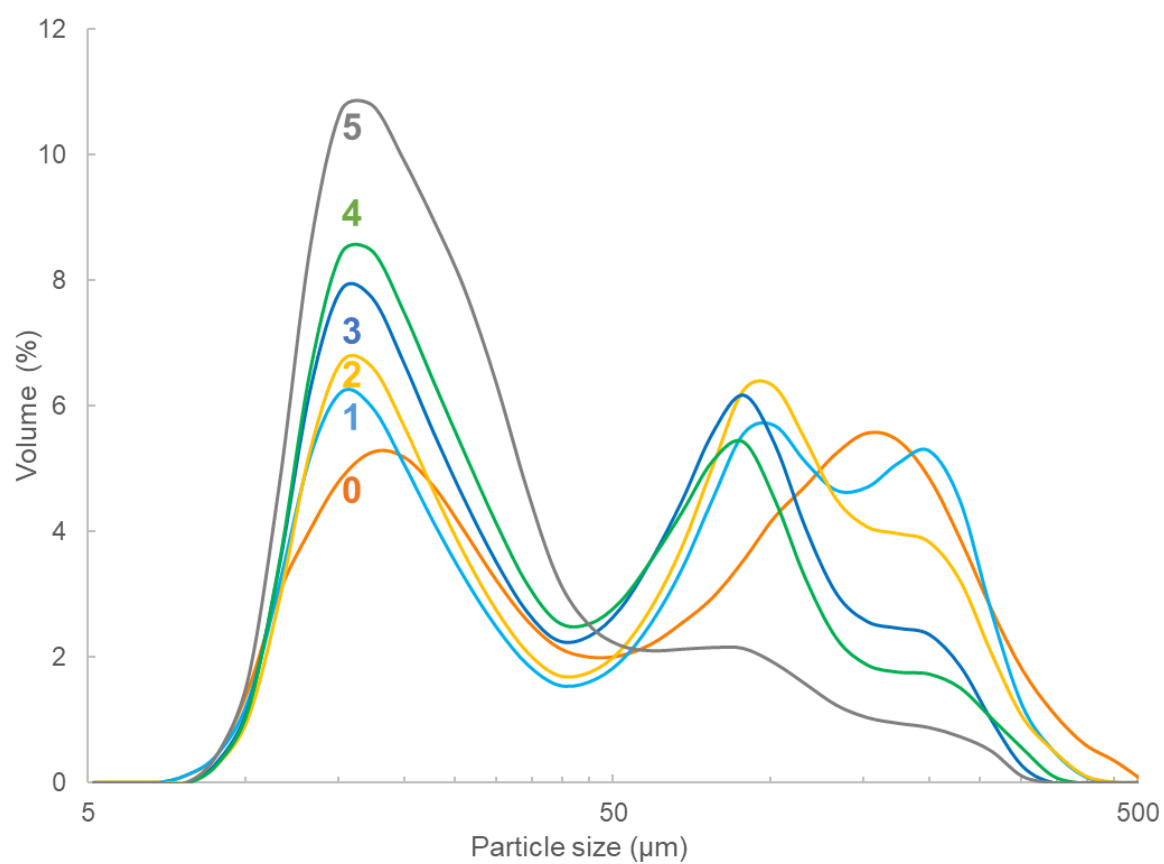
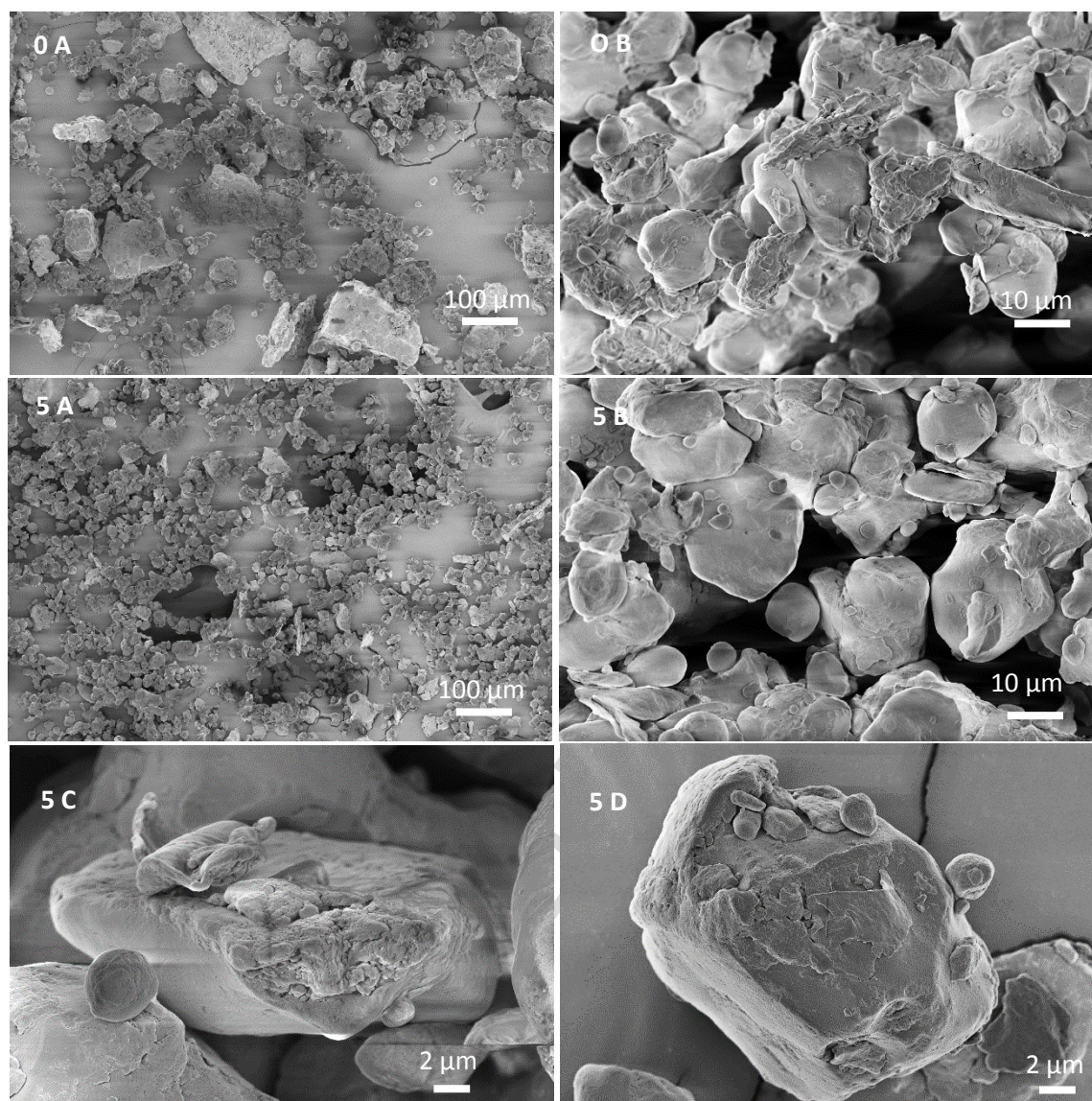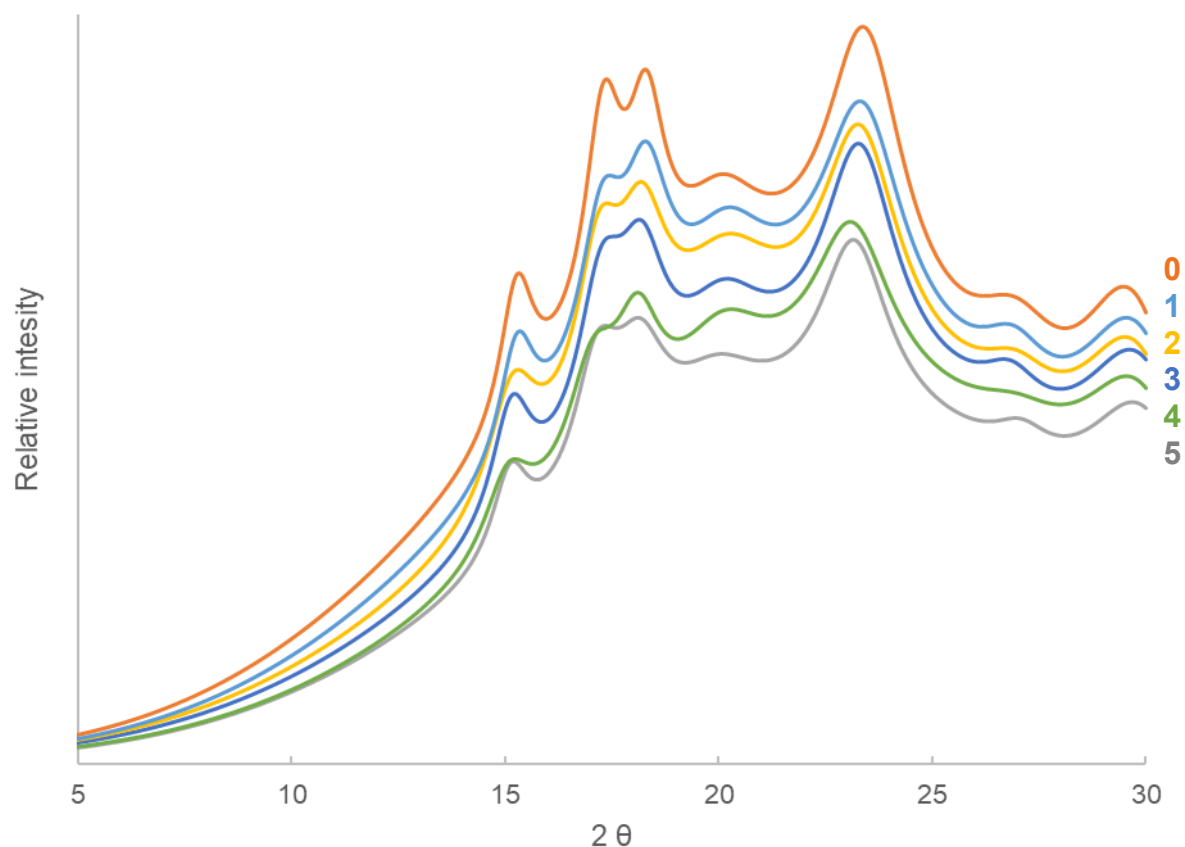Fig. 2. SEM images of untreated sorghum flour (0= no treatment) and highly milled sample (5 = 5.84 kJ/g).
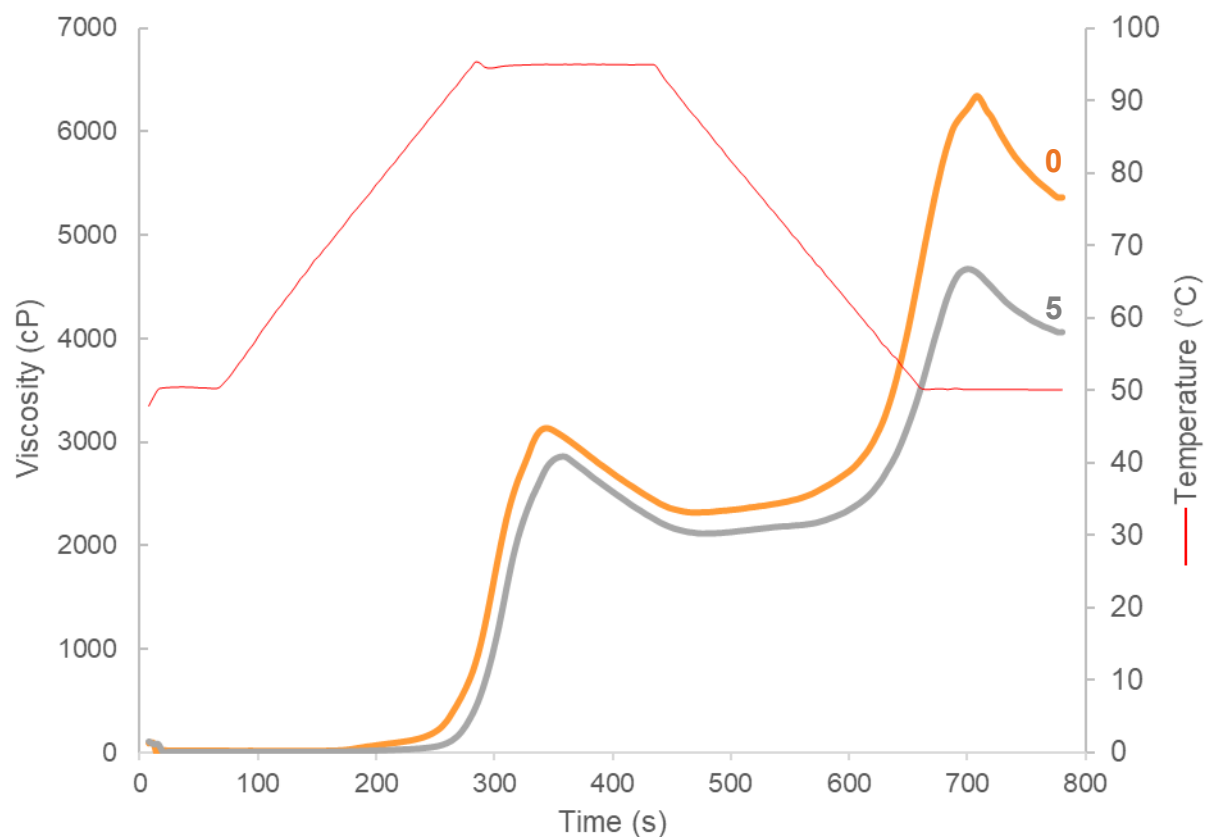
Fig 3. X-ray diffraction pattern (WAXS) of planetary ball milled sorghum flour as a function of milling energy (0= no treatment, 1 = 0.26 kJ/g, 2 = 0.99 kJ/g, 3 = 1.96 kJ/g, 4 = 2.93 kJ/g, 5 = 5.84 kJ/g).

1 Fig. 4. Pasting profile of planetary milled sorghum flour (0= no treatment and 5 = 5.84 kJ/g)

2

3

Highlights

Planetary ball milling decreased the particle size of sorghum flour

Milling energy increased damaged starch content and decreased final viscosity and setback

Gelatinization enthalpy and crystallinity degree decreased with increasing milling energy